

Estimation of the cortical functional connectivity with the multimodal integration of high-resolution EEG and fMRI data by directed transfer function

F. Babiloni,^{a,b,*} F. Cincotti,^b C. Babiloni,^{a,c,d} F. Carducci,^{a,c,d} D. Mattia,^b L. Astolfi,^{b,e}
A. Basilisco,^a P.M. Rossini,^{c,d,f} L. Ding,^{g,h} Y. Ni,^g J. Cheng,^g K. Christine,^g
J. Sweeney,^g and B. He^{g,h}

^aDepartment of Human Physiology and Pharmacology, University “La Sapienza”, Rome, Italy

^bIRCCS Fondazione Santa Lucia, Rome, Italy

^cAFAR-Department of Neuroscience, Ospedale Isola Tiberina, Rome, Italy

^dIRCCS “Centro S. Giovanni di Dio-Fatebenefratelli”, Brescia, Italy

^eDepartment of Informatics and Systems, University “La Sapienza”, Rome, Italy

^fDepartment of Neurology, University Campus Bio-Medico, Rome, Italy

^gUniversity of Illinois, Chicago, IL 60607, USA

^hUniversity of Minnesota, Minneapolis, MN 55455, USA

Received 2 March 2004; revised 17 May 2004; accepted 23 September 2004
Available online 13 November 2004

Nowadays, several types of brain imaging device are available to provide images of the functional activity of the cerebral cortex based on hemodynamic, metabolic, or electromagnetic measurements. However, static images of brain regions activated during particular tasks do not convey the information of how these regions communicate with each other. In this study, advanced methods for the estimation of cortical connectivity from combined high-resolution electroencephalography (EEG) and functional magnetic resonance imaging (fMRI) data are presented. These methods include a subject’s multicompartiment head model (scalp, skull, dura mater, cortex) constructed from individual magnetic resonance images, multidipole source model, and regularized linear inverse source estimates of cortical current density. Determination of the priors in the resolution of the linear inverse problem was performed with the use of information from the hemodynamic responses of the cortical areas as revealed by block-designed (strength of activated voxels) fMRI. We estimate functional cortical connectivity by computing the directed transfer function (DTF) on the estimated cortical current density waveforms in regions of interest (ROIs) on the modeled cortical mantle. The proposed method was able to unveil the direction of the information flow between the cortical regions of interest, as it is directional in nature. Furthermore, this method allows to detect changes in the time course of information flow between cortical regions in different frequency bands. The reliability of these techniques was further demonstrated by elaboration of high-resolution

EEG and fMRI signals collected during visually triggered finger movements in four healthy subjects. Connectivity patterns estimated for this task reveal an involvement of right parietal and bilateral premotor and prefrontal cortical areas. This cortical region involvement resembles that revealed in previous studies where visually triggered finger movements were analyzed with the use of separate EEG or fMRI measurements.

© 2004 Elsevier Inc. All rights reserved.

Keywords: Linear inverse source estimate; EEG and fMRI integration; Movement-related potentials; DTF; Finger tapping

Introduction

Nowadays, there are several types of brain imaging device that are able to provide images of the functional activity of the cerebral cortex based on hemodynamic, metabolic, or electromagnetic measurements. However, static images of brain regions activated during particular tasks do not convey a sufficient amount of information with respect to the central issue of how these regions communicated with each other. The concept of brain connectivity now plays a central role in neuroscience as a way to understand one possible ‘code’ of the functioning brain, as well as the organized behavior of cortical regions beyond the simple mapping of their activity (David et al., 2004; Horwitz, 2003; Lee et al., 2003). Different approaches for the estimate of cortical connectivity have already been exploited in the literature based on

* Corresponding author. Dipartimento di Fisiologia Umana e Farmacologia, Università di Roma “La Sapienza”, P.le A. Moro 5, 00185 Roma, Italy. Fax: +39 6 49910917.

E-mail address: Fabio.Babiloni@uniroma1.it (F. Babiloni).

Available online on ScienceDirect (www.sciencedirect.com).

hemodynamic or metabolic measurements (Buchel and Friston, 1997), electroencephalography (EEG) scalp potentials (Brovelli et al., 2002; Gevins et al., 1989; Urbano et al., 1998), and magnetoencephalographic (MEG) fields (Taniguchi et al., 2000).

Structural equation models have been used to investigate cortical connectivity in the human brain by means of functional magnetic resonance imaging (fMRI, Buchel and Friston, 1997; McIntosh and Gonzalez-Lima, 1994; Schlosser et al., 2003). However, the temporal dynamics of the hemodynamic process (on the scale of seconds) makes it problematic to follow the transient activity of the neural populations that develops in the order of tens of milliseconds. Indeed, EEG and MEG are known as useful techniques for the study of brain dynamics due to their high temporal resolution (milliseconds; Nunez, 1981, 1995). However, in the EEG case, the different electrical conductivities of the brain, skull, and scalp markedly blur the EEG potential distributions and render the localization of the underlying cortical generators problematic. In last decade, techniques known as high-resolution EEG had allowed to estimate precisely the cortical activity from noninvasive EEG measurements (Babiloni et al., 1997; Gevins, 1989, 1991, 1999; He and Lian, 2002; He et al., 2002; Nunez, 1995). This body of EEG techniques includes the use of a large number of scalp electrodes, realistic models of the head derived from structural magnetic resonance images (MRIs), and advanced processing methodologies related to the solution of the linear inverse problem. These methodologies allow the estimation of cortical current density from sensor measurements (Babiloni et al., 2000; Grave de Peralta Menendez and Gonzalez Andino, 1999; Pascual-Marqui, 1995). Nowadays, all the connectivity estimations performed on cerebral electromagnetic signals have been computed between the signals gathered from the electric or magnetic sensors (Gevins et al., 1989; Urbano et al., 1998). On the other hand, the relation between the observed spatial patterns in the sensor space and those in the source space is complicated by the spreading of the potential from the cortex to the sensors. Recently, a methodology being able to compute the coherence between cortical areas has been introduced, and applications to MEG data gathered from normal and Parkinson's disease patients were provided (Gross et al., 2001, 2003). This methodology was applied to cortical signals estimated from MEG measurements, thus improving the spatial details available with respect to the computation of coherence from signals derived directly from the sensors. However, in this case, the direction of the information flow between the cortical areas was not available due to the nondirectional nature of coherence computation.

Here, we present a novel computational approach for the estimation of cortical connectivity based on directed transfer function (DTF), a technique used to estimate the direction of information flow between signals gathered from EEG sensors (Kaminski and Blinowska, 1991; Kaminski et al., 2001). We applied the DTF approach on the cortical signals estimated from high-resolution EEG recordings by using realistic head models and a cortical reconstruction algorithm on an average of 5000 dipoles uniformly disposed along the cortical surface. The estimation of the cortical activity was obtained by application of the linear inverse procedure (Grave de Peralta Menendez and Gonzalez Andino, 1999; Pascual-Marqui, 1995). In this estimation procedure, several a priori information were used in order to increase the quality of the cortical current density

estimates. The first a priori information used was the anatomical constraints by placing the current dipoles orthogonally to the reconstructed cortical surface. An additional constraint was to force the dipoles to explain the recorded data with a minimum or a low amount of energy (minimum-norm solutions; Dale and Sereno, 1993; Hämäläinen and Ilmoniemi, 1984).

The solution space can be further reduced by using information derived from hemodynamic measures (i.e., fMRI-BOLD phenomenon) recorded during the same task. The rationale of this multimodal approach is that neural activity, modulating neuronal firing and generating synchronized and coherent EEG potentials, increases glucose and oxygen demands (Dale et al., 2000; Liu et al., 1998; Magistretti et al., 1999). This results in an increase in the local hemodynamic response that can be measured by fMRI (Grinvald et al., 1986; Puce et al., 1997). Hence, fMRI responses and cortical sources of EEG data can be spatially related (Logothetis et al., 2001). Furthermore, numerical simulations have shown that the use of fMRI priors increases the quality of the cortical current estimations (Babiloni et al., 2003; Liu, 2000, 1998). In the present study, this integrated approach is proposed for the estimation of cortical connectivity from combined electromagnetic and hemodynamic measurements in humans, and tested by analyzing visually paced finger movements executed by four healthy subjects.

Methods

Subject and experimental design

Four normal right-handed subjects (one male, three females; mean age 23 ± 0.2 years) participated in the study after informed consent was obtained, according to the Institutional Review Board at the University of Illinois at Chicago. Subjects were seated comfortably in an armchair with both arms relaxed and resting on pillows and were requested to perform fast repetitive right finger movements that were cued by visual stimuli. Ten to fifteen blocks of 2-Hz thumb oppositions for right hands were recorded with each 30-s blocks of finger movement and rest. During the movement, subjects were instructed to avoid eye blinks, swallowing, or any movement other than the required finger movements.

High-resolution EEG recordings

Event-related potential (ERP) data were recorded with 96 electrodes; data were recorded with a left ear reference and submitted to the artifact removal processing. Six hundred ERP trials of 600 ms of duration were acquired. A/D sampling rate was 250 Hz. The surface electromyographic (EMG) activity of the muscle was also collected. The onset of EMG response served as zero time. All data were visually inspected, and trials containing artifacts were rejected. We use semiautomatic supervised threshold criteria for the rejection of trials contaminated by ocular and EMG artifacts, as described in details elsewhere (Moretti et al., 2003). After the EEG recording, the electrode positions were digitized using a three-dimensional localization device with respect to the anatomic landmarks of the head (nasion and two preauricular points). The MRIs of each subject's head were also acquired. These

images were used for the construction of the individual realistic geometry head model. The realistic head models are necessary for the estimation of cortical activity in the appropriate region of interest (ROIs) by using the linear inverse procedure algorithms from the scalp-recorded ERP data. The time-varying spectral values of the estimated cortical activity in the theta (4–7 Hz), alpha (8–12 Hz), beta (13–30 Hz), and gamma (30–45 Hz) frequency bands were also computed in each defined ROI. The analysis period for the potentials time locked to the movement execution was set from 300 ms before to 300 ms after the EMG trigger (0 time); the ERP time course was divided in two phases relative to the EMG onset; the first, labeled as “PRE” period, marked the 300 ms before the EMG onset and was intended as a generic preparation period; the second labeled as “POST” lasted up to 300 ms after the EMG onset and was intended to signal the arrival of the movement somatosensory feedback. We maintained the same PRE and POST nomenclature for the signals estimated at the cortical level.

fMRI data acquisition

All fMRI studies were performed on a 3.0-T scanner (General Electric Medical Systems, Milwaukee, WI) with BOLD echo planar imaging (EPI) capability (Advanced NMR Systems Inc., Wilmington, MA). Gradient echo EPI, sensitive to the BOLD effects, was performed using a commercial quadrature birdcage radio frequency coil.

Subjects’ heads were laid comfortably within the head coil and firm cushions were used to minimize the head motion. Forty axial (horizontal) slices with coverage of the whole brain were acquired. Acquisition parameters used in the functional scans were TE = 25 ms, TR = 3 s, flip angle = 90°; 3 mm slice thickness with 0 mm gap; 64 × 64 acquisition matrix with a field of view (FOV) of 20 × 20 cm. The subjects were asked to perform the fast repetitive finger movement in the following sequence within one scan session: fixation (30 s), right hand finger movements (30 s). The sequence was repeated five times during a single scan session. High-resolution structural images were also acquired in the axial plane [three-dimensional spoiled gradient recalled imaging (SPGR)] with 1.9 mm thick contiguous slices for two subjects; 2 and 1.8 mm thick were used for the remaining two subjects, respectively.

Head and cortical models

Subjects’ realistic geometry head models reconstructed from T1-weighted MRIs were employed. The scalp, skull, and dura mater compartments were segmented from MRIs and triangulated with about 1000 triangles for each surface. The source model was built with the following procedure: (i) the cortex compartment was segmented from MRIs and triangulated obtaining a fine mesh with about 100,000 triangles; (ii) a coarser mesh was obtained by resampling the fine mesh previously described to about 5000 triangles. This was done by preserving the general features of the neocortical envelope, especially in correspondence of pre- and post-central gyri and frontal mesial area; (iii) an orthogonal unitary equivalent current dipole was placed in each node of the triangulated surface, with direction parallel to the vector sum of the normals to the surrounding triangles.

Estimation of cortical source current density

The solution of the following linear system

$$\mathbf{A}x = b + n \quad (1)$$

provides an estimation of the dipole source configuration x that generated the measured EEG potential distribution b . The system also includes the measurement noise n , supposed normally distributed.

Also, in Eq. (1), \mathbf{A} is the lead field matrix, in which each j th column describing the potential distribution generated on the scalp electrodes by the j th unitary dipole. The current density solution vector ξ was obtained as (Grave de Peralta Menendez and Gonzalez Andino, 1999):

$$\xi = \underset{x}{\operatorname{argmin}} (\|\mathbf{A}x - b\|_{\mathbf{M}}^2 + \lambda^2 \|x\|_{\mathbf{N}}^2) \quad (2)$$

where \mathbf{M} and \mathbf{N} are the matrices associated to the metrics of the data and of the source space, respectively, λ is the regularization parameter, and $\|x\|_{\mathbf{M}}$ represents the \mathbf{M} norm of the vector x . The solution of Eq. (2) is given by the inverse operator \mathbf{G} as follows:

$$\xi = \mathbf{G}b, \mathbf{G} = \mathbf{N}^{-1}\mathbf{A}'(\mathbf{A}\mathbf{N}^{-1}\mathbf{A}' + \lambda\mathbf{M}^{-1})^{-1} \quad (3)$$

An optimal regularization of this linear system was obtained by the L-curve approach (Hansen, 1992a,b). As a metric in the data space we used the identity matrix, while as a norm in the source space we used the following metric that takes into account the hemodynamic information offered by the recorded fMRI data

$$(\mathbf{N}^{-1})_{ii} = g(\alpha_i)^2 \|\mathbf{A}_{\cdot i}\|^{-2} \quad (4)$$

where $(\mathbf{N}^{-1})_{ii}$ is the i th element of the inverse of the diagonal matrix \mathbf{N} and all the other matrix elements \mathbf{N}_{ij} are set to 0. The L_2 norm of the i th column of the lead field matrix \mathbf{A} is denoted by $\|\mathbf{A}_{\cdot i}\|$. The $g(\alpha_i)$ is a function of the statistically significant percentage increase of the fMRI signal during the task compared to the rest state. Such function has values greater than 1 for positive α_i , while takes values lower than 1 for negative α_i . In particular, such function is defined as

$$g(\alpha) = \max \left\{ 1 + (K - 1) \frac{\alpha_i}{\max_i \{\alpha_i\}}, 1/K \right\}, \quad K \geq 1, \forall \alpha \quad (5)$$

where the value of the parameter K tunes the strength of the inclusion of the fMRI constraints in the source space and the function $\max(a,b)$ takes the maximum of the two arguments for each α . Here, we used the value of $K = 10$ that resulted from a previous simulation study, as a value returning optimal estimation of source current density with fMRI priors for a large range of SNR values of the gathered EEG signals (Babiloni et al., 2003).

Regions of interest

Several cortical regions of interest (ROIs) were drawn by two independent and expert neuroradiologists on the computer-based cortical reconstruction of the head models obtained for the four experimental subjects. In particular, the ROIs representing the left and right primary somatosensory cortex (S1) included the Brodmann areas (BA) 3, 2, 1, whereas the ROIs representing the left and right primary motor cortex (MI) included the BA 4. The ROIs representing the supplementary motor area (SMA) were

obtained from the cortical voxels belonging to BA 6. We further separated the proper and anterior SMA indicated with BA 6P and 6A, respectively. Furthermore, ROIs from the right and the left parietal associative areas, including BA 5 and 7, and the bilateral occipital area (BA 19), were also considered. In the frontal regions, BA 46, 8, and 9 were bilaterally selected.

Cortical-estimated waveforms

By using the relations described in Eqs. (1)–(4), at each time point of the gathered ERP data, an estimate of the signed magnitude of the dipolar moment for each one of the 5000 cortical dipoles was obtained. In fact, since the orientation of the dipole was already defined to be perpendicular to the local cortical surface of the model, the estimation process returned a scalar rather than a vector field. In order to obtain the cortical current waveforms for all the time points of the recorded EEG time series, we used a unique “quasi-optimal” regularization λ value for all the analyzed EEG potential distributions. Such quasi-optimal regularization value was computed as an average of the several λ values obtained by solving the linear inverse problem for a series of EEG potential distributions. These distributions are characterized by an average global field power (GFP) with respect to the higher and lower GFP values obtained during all the recorded waveforms. The instantaneous average of the dipole’s signed magnitude belonging to a particular ROI generates the representative time value of the cortical activity in that given ROI. By iterating this procedure on all the time instants of the gathered ERP, the cortical ROI current density waveforms were obtained, and they could be taken as representative of the average activity of the ROI during the task performed by the experimental subjects. These waveforms could then be subjected to the following processing in order to estimate the connectivity pattern between ROIs.

Statistical parametric mapping

What is often missing in EEG linear inverse solutions is the level of reliability of the solution itself. Not all modeled sources have the same degree of sensitivity to the measurement noise, so we cannot say whether a source has a high strength because it is the most probable source of that potential distribution, or just because that source accounts well for the noise superimposed to the potential. Even in the ideal case of the absence of noise, some sources seem more inclined to explain a large set of data, just because of their geometrical properties (i.e., sources positioned on a gyrus close to a cortical convexity, rather than deep in a sulcus). A statistical approach to the problem and a measure of the signal to noise ratio in the modeled cortical activity are then required. The level of noise in the EEG linear inverse solutions can be addressed by estimating the “projection” of the EEG noise $n(t)$ onto the cortical surface by means of the computed pseudoinverse operator \mathbf{G} ; the standard error of the noise on the estimated source strength ξ_j is given by

$$\langle \mathbf{G}_j \cdot n(t) \rangle = \mathbf{G}_j \cdot \mathbf{C}(\mathbf{G}_j)' \quad (6)$$

where \mathbf{G}_j is the j th row of the pseudoinverse matrix, \mathbf{C} is the EEG noise covariance matrix ($\mathbf{C}_{ij} = \langle n_i(t), n_j(t) \rangle$). This allows to quantitatively assess the ratio between the estimated cortical activity x and the amount of noise at the cortical level, quantified through the standard deviation of its estimate (Dale et al., 2000). It

can be demonstrated that under the hypothesis of a normal estimate for the noise $n(t)$ obtained with more than 50 time points, the following normally distributed z score estimator can be obtained for each j th cortical location and for each time point t considered

$$z_j(t) = \frac{\mathbf{G}_j \cdot b(t)}{\sqrt{\mathbf{G}_j \cdot \mathbf{C}(\mathbf{G}_j)'}} \quad (7)$$

where \mathbf{C} is the estimated noise covariance matrix. The uncorrected threshold for the z score level at 5% is 1.96. Values of z exceeding such threshold represent levels of estimated cortical activity that are unlikely due to the chance alone but are related to the task performed by the experimental subject. However, to avoid the effects of the increase of the Type I error due to the multiple z tests performed, the results will be presented after the application of the Bonferroni correction (Zar, 1984).

Directed transfer function

The directed transfer function (DTF) technique (Kaminski and Blinowska, 1991) is a full multivariate spectral measure used to determine directional influences between any given pair of signals in a multivariate data set. It is computed on a multivariate autoregressive model (MVAR) that simultaneously models the whole set of signals. DTF has been demonstrated (Kaminski et al., 2001) to be based on the concept of Granger causality, according to which an observed time series $s_1(n)$ can be said to cause another time series $s_2(n)$ if the prediction error for $s_2(n)$ at the present time is reduced by the knowledge of $s_1(n)$ ’s past measurements. This kind of relation is not reciprocal, thus allowing to determine the direction of information flow between the time series.

In this study, the DTF technique was then applied to the set of cortical estimated waveforms S

$$S = [s_1(t), s_2(t), \dots, s_N(t)]^T \quad (8)$$

obtained for the N ROIs considered. The following MVAR process is an adequate description of the data set S :

$$\sum_{k=0}^p A(k)S(t-k) = \mathbf{E}(t) \quad \text{with } A(0) = 1 \quad (9)$$

under the condition in which $\mathbf{E}(t)$ is a vector of multivariate zero-mean uncorrelated white noise process. In Eq. (9), A_1, A_2, \dots, A_p are the $\mathbf{N} \times \mathbf{N}$ matrices of model coefficients while p is the model order chosen with the Akaike information criteria (AIC) for MVAR process (Kaminski et al., 2001). In order to investigate the spectral properties of the examined process, Eq. (9) is transformed to the frequency domain:

$$A(f)S(f) = \mathbf{E}(f) \quad (10)$$

where

$$A(f) = \sum_{k=0}^p A(k)e^{-j2\pi f A k} \quad (11)$$

Eq. (10) can be then rewritten as

$$S(f) = A^{-1}(f)\mathbf{E}(f) = H(f)\mathbf{E}(f). \quad (12)$$

$H(f)$ is the transfer matrix of the system, whose element H_{ij} represents the connection between the j th input and the i th output of the system. With these definitions, the causal influence of the

cortical waveform estimated in the j th ROI on that estimated in the i th ROI (the directed transfer function $\theta_{ij}^2(f)$) is defined as:

$$\theta_{ij}^2(f) = |H_{ij}(f)|^2. \quad (13)$$

In order to be able to compare the results obtained for cortical waveforms with different power spectra, a normalization was performed by dividing each estimated DTF by the squared sums of all elements of the relevant row, thus obtaining the so-called normalized DTF (Kaminski and Blinowska, 1991):

$$\gamma_{ij}^2(f) = \frac{|H_{ij}(f)|^2}{\sum_{m=1}^N |H_{im}(f)|^2} \quad (14)$$

$\gamma_{ij}(f)$ expresses the ratio of influence of the cortical waveform estimated in the j th ROI on the cortical waveform estimated on the i th ROI with respect to the influence of all the estimated cortical waveforms. Normalized DTF values are in the interval [0,1] when the normalization condition

$$\sum_{n=1}^N \gamma_{in}^2(f) = 1 \quad (15)$$

is applied.

Statistical evaluation of connectivity measurements

As DTF functions have a highly nonlinear relation to the time series data from which they are derived, the distribution of their estimators is not well established. This makes tests of significance difficult to perform. A possible solution to this problem was recently proposed in Kaminski et al. (2001). It consists of the use of a surrogate data technique (Theiler et al., 1992), in which one generates an empirical distribution for a given estimator when interactions between signals are removed. Significance tests based on this empirical distribution can then be performed. Specifically, one randomly and independently shuffles the time series data from each ROI to create a surrogate data set. A bivariate autoregressive model is then fit to the shuffled data and the DTF functions are computed from such model. Carrying out this process many times, each time performed on an independently shuffled data set, it is possible to construct an empirical distribution for the DTF functions. Since the shuffling procedure destroys all the temporal structure in the data, this empirical distribution gives the variability for the DTF functions for the null hypothesis case. Using this distribution, one can then assess the significance of the causal measures evaluated from the actual data. Without having an explicit formulation for the shape of this distribution, one can thus compute an empirical threshold for a given significance level. A limit of this method is due to the fact that it destroys interdependency among time series as well as the temporal structure within a time series. In fact, in the above-mentioned procedure, samples from all the frequencies are combined into a single distribution, which is independent from frequency and gives a single threshold for all the DTF values. In order to randomize the sequential order while preserving the correlation structure, we adopted a variation of this method. The surrogate data set was created by shuffling the trials within each series, without shuffling single samples within a trial. In this way, we

preserved the spectral properties of the time series, thus being able to obtain a distribution for each frequency value and a consequently threshold dependent from frequency. The shuffling procedure was performed for 1000 times and the statistical significance level was set to 0.01%.

Connectivity inflow–outflow relationships

The connectivity patterns in the different frequency bands between the different cortical regions were summarized by using appropriate indexes representing the total flow from and toward the selected cortical area. In particular, we defined the total inflow in a particular cortical region as the sum of the statistically significant connections (with their values) from all the other cortical regions toward the selected area. The total inflow for each ROI is represented by a sphere centered on the cortical region, whose radius is linearly related to the magnitude of all the incoming statistically significant links from the other regions. Such information is also coded through a color scale. Such information depicts the ROI as target of functional connections from the other ROIs. Same conventions are used to represent the total outflow from a cortical region toward the others, generated by the sum of all the statistical significant links obtained by application of the DTF to the cortical waveforms (with their values).

Results

A selection of the gathered ERPs related to the visually paced right finger tapping task performed by Subject #1 is shown on the upper panel of Fig. 1. These waveforms are relative to the signals gathered from the standard electrode leads of the augmented 10–20 international system that are represented on the realistic geometry scalp reconstruction of the subject (center of the figure). The waveforms shown resulted from the average of the artifact-free trials aligned on the EMG onset. Hemodynamic fMRI data collected from all the subjects served as a priori information to constrain the solution of the linear inverse problem, in the way described above by Eqs. (1)–(5). Using the linear inverse procedure, the estimation of the current density waveforms for the selected ROIs was then obtained. In order to define the statistical significance of these cortical estimated waveforms, the z score transformation was applied following Eqs. (6) and (7). The estimated z score waveforms are represented for some selected ROIs in the bottom panel of Fig. 1 (Subject #1). Note that the z score scale of the waveforms ranges from 0 (the baseline) to 10; this latter value corresponding to a level of statistical significance equal to $P < 10^{-7}$. The use of a high values of z score is appropriate, since the uncorrected level for statistical significance of the estimated waveforms is only equal to 1.96 ($P < 5 \times 10^{-2}$). However, we used an increased level of statistical significance to discuss the obtained data ($z = 5$, $P < 10^{-5}$) in order to avoid the risks of the so-called alpha inflation (Abt, 1983). This alpha inflation is related to the increase of the probability to get significant results by chance alone, due to the execution of multiple univariate tests. Cortical activity was significantly different from baseline in the left ROIs representing parietal (BA 5), premotor (BA 6A), sensorimotor (BA 3, 2, 1, BA 4), and prefrontal (BA 8 and BA 9) cortical areas, whereas a similar statistical engage has been observed on the right hemisphere only for the ROIs corresponding to premotor (BA 6A) and prefrontal (BA 8) cortical areas.

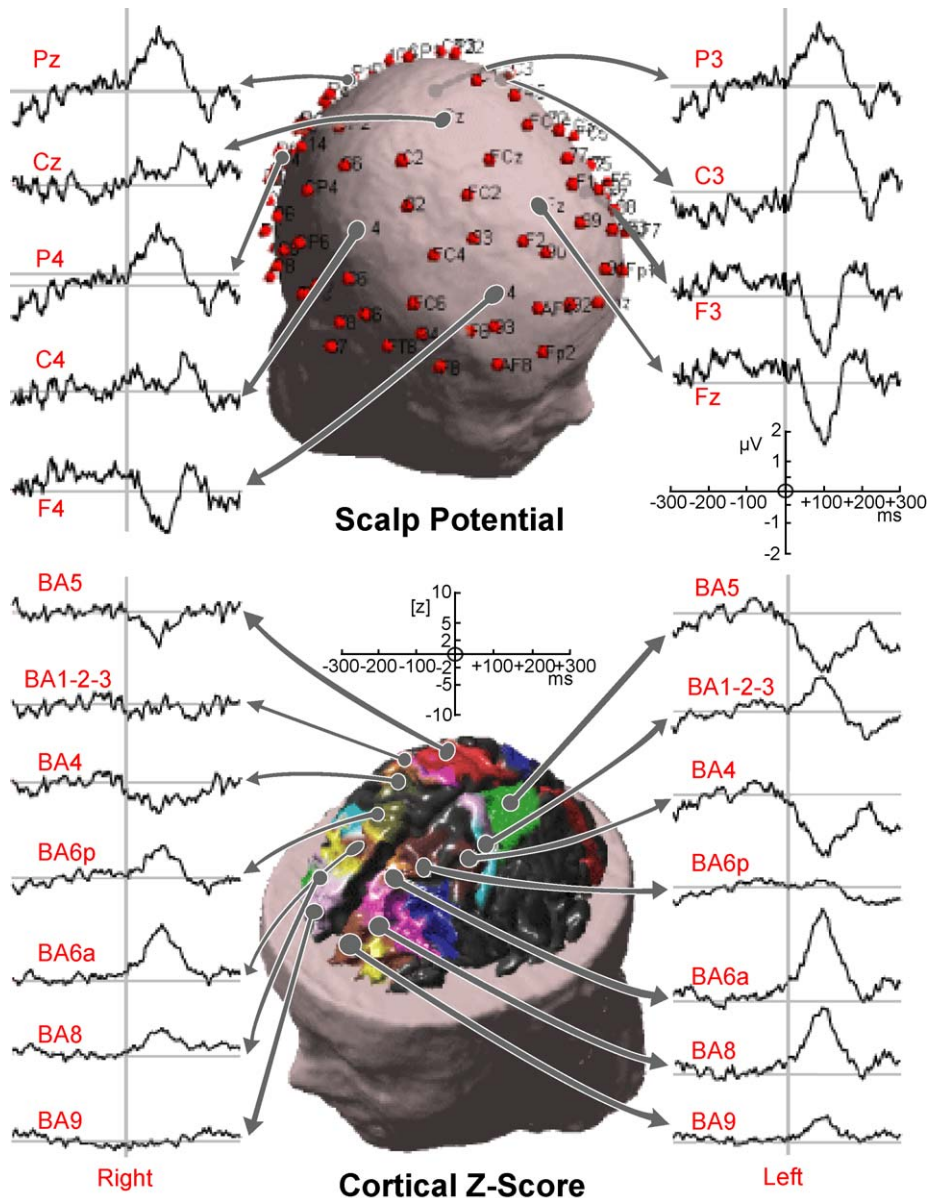


Fig. 1. (Top panel) Selection of the ERPs gathered during the visually paced right finger tapping performed by Subject #1. The ERP waveforms are relative to the signals gathered from the standard electrode leads of the augmented 10–20 international system, represented on the realistic scalp reconstruction of the subject at the center of the figure. The waveforms are relative to the average of the artifact-free trials, and the gray vertical bar indicates the onset of the EMG trigger, located 300 ms from the beginning of the ERP waveform. (Bottom panel) Estimates of the statistical significance of the cortical activity in selected ROIs depicted on the realistic representation of the cortex in Subject #1. Such estimation was performed first by estimating the cortical activity with the use of the a priori information from the hemodynamic measurements during the solution of the linear inverse problem. Then, in order to obtain the statistical significance of cortical estimated waveforms, the z score transformation was first applied and then represented. Note the z score scale of the waveforms, ranging from 0 (the baseline) to 10; this latter value corresponding to a level of statistical significance equal to $P < 10^{-7}$. The figure at the center shows the different ROIs drawn on different colors on the cortical surface reconstruction of Subject #1.

Connectivity analysis

The task-related pattern of cortical connectivity was obtained by applying the DTF methodology to the cortical current density waveforms estimated in each particular ROI depicted on the realistic geometry head model. The connectivity patterns between the ROIs have been represented by arrows pointing from one cortical area (“the source”) toward another one (“the target”). The color and size of the arrows code the strength level of the functional connectivity observed between the source and

the target ROI. The labels on the cortical reconstruction of the brain indicate the names of the ROIs involved in the estimated connectivity pattern. Furthermore, we summarized the behavior of a ROI as a sink for the information flow from the other ROIs by adding all the value of the links reaching a particular ROI from all the others. The information is represented with the size and the color of a sphere, centered on the particular ROI analyzed; the larger the sphere, the higher the value of inflow or outflow of a given ROI. Fig. 2 shows the connectivity patterns estimated in the theta band during the POST time

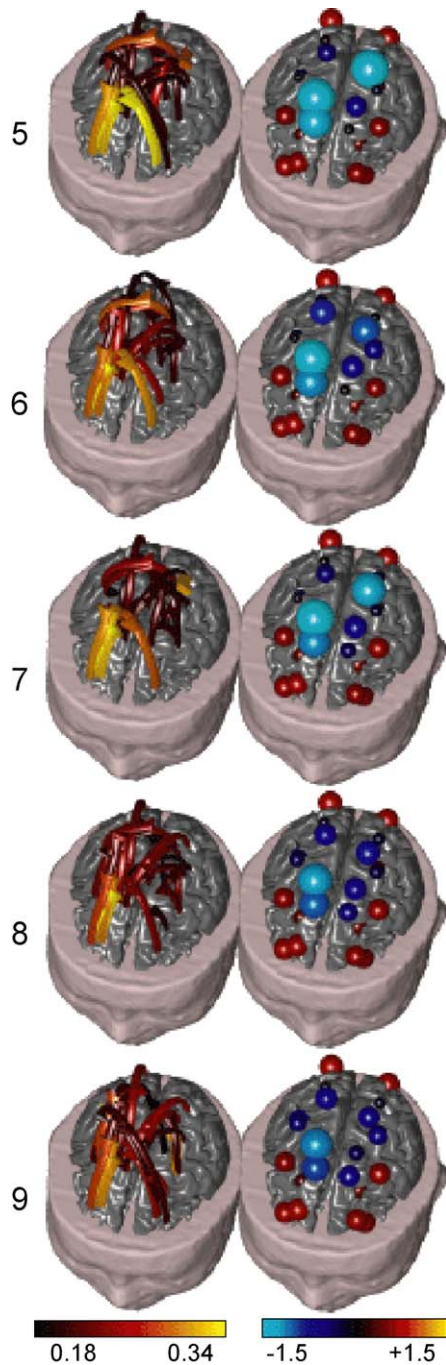


Fig. 3. (Left column) Connectivity patterns related to the different model orders used for the MVAR of the finger tapping data, starting from the order 5 (top) to the order 9 (low). (Right column) Inflow (red hues) and outflow (blue hues) patterns related to the same different model orders for the MVAR. Note the similarity of the computed connectivity patterns, which is rather independent from the correct estimation of the order for the MVAR process.

and with both the prefrontal ROIs. The stronger functional connections are relative to the link between the premotor and prefrontal areas of both cerebral hemispheres. After the preparation and the beginning of the finger movement (POST period), the connectivity patterns slightly changed in all the subjects examined. As for the beta frequency band, the connectivity patterns for the

overall subjects did not differ from those obtained for the alpha band (data not shown). Conversely, the connectivity patterns in the gamma frequency band displayed an involvement of the right parietal (BA 5), motor (BA 4), and premotor cortical areas (BA 6) as a source of links spreading toward the left sensorimotor and parietal cortical areas in the analyzed subjects (Fig. 5).

Fig. 6 shows the inflow and outflow patterns computed for the alpha frequency band in all the considered ROIs and obtained for the PRE and POST periods of all subjects. The ROIs, which are very active as sink (i.e., the target of the information flow from other ROIs), result generally stable with respect to the PRE and POST periods. Indeed, the major sink ROIs are located in the parietooccipital areas (including the bilateral BA 19 and 7) and in the premotor and the prefrontal areas (including the bilateral BA 8, 9, and 6) for all the examined subjects. The most active ROIs functioning as a source during the same time periods are generally located in the right parietal (BA 5) and in the primary motor area (BA 4). Similar

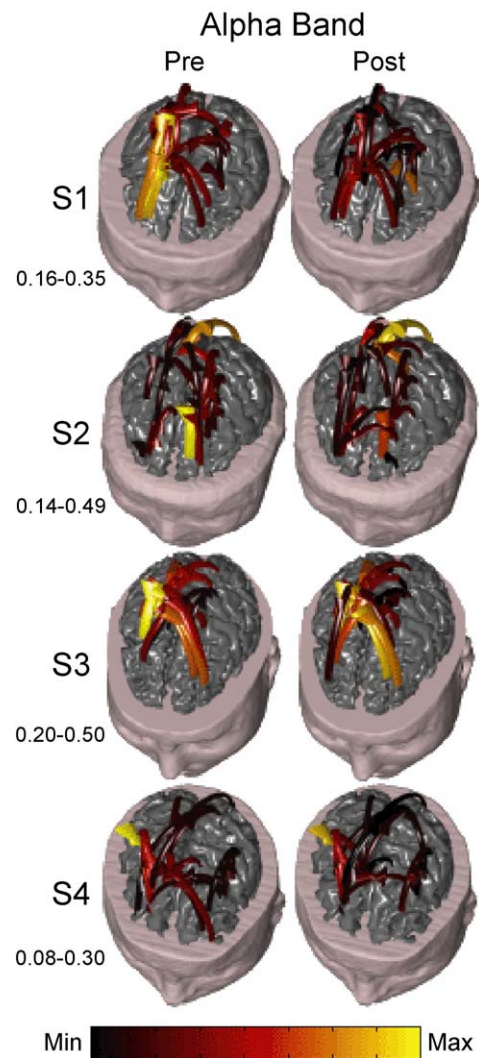


Fig. 4. Connectivity patterns estimated in the alpha frequency band by application of DTF methodology on the estimated cortical waveforms in the four subjects analyzed. The connectivity estimates are relative to the period before EMG onset (PRE label, first column) and from the EMG to the end of recordings (POST label, second column). After preparation and beginning of finger movements (POST period), the connectivity patterns slightly changed in all the subjects examined.

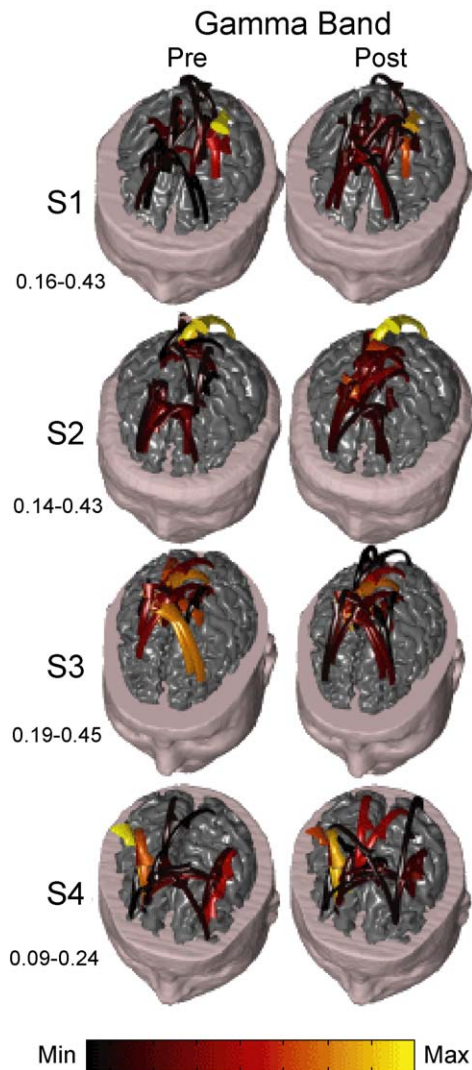


Fig. 5. Connectivity patterns estimated for the gamma frequency band in all subjects. Same conventions applied as in Fig. 4.

to what was observed for cortical connectivity patterns, the inflow and the outflow patterns relative to the beta frequency bands were resembling those presented for the alpha band. As shown in Fig. 7, we found that in the gamma band range the situation was slightly different: the main targets of the functional connections spreading from the right parietal and premotor cortical areas (see the outflow pattern on the third and fourth column of the figure) are the occipital as well as the prefrontal cortical areas of both hemispheres (BA 19, BA 8, 9, and 46).

Discussion

Methodological considerations

We have presented a body of techniques to unveil changes in functional connectivity between cortical ROIs, depicted on realistic geometry models of the head volume conductor, based on high-resolution EEG data. The connectivity estimations have been performed on ROIs depicted along Brodman areas (BAs) identified on individual cortical model. This strategy uses a priori informa-

tion according to the role of the BAs in the brain functions. The presented technique could also be applied by drawing the ROIs around the cortical estimated peaks of the power spectra activity in the different frequency bands with a post hoc procedure (Gross et al., 2001). Here, we have rather employed the ROIs depicted on the base of the BAs to allow comparison of the functional connectivity patterns elicited by the same experimental behavior across subjects.

The present analysis was based on a cortical source model, namely the source space where the cortical activity generates was identified by estimating the inverse operator \mathbf{G} relative to the realistic geometry of the cortical surface of each subject. Hence, it may be argued that since only cortical sources are modeled, if a deep source is active then the source reconstruction (and likely the connectivity estimates) could fail. In this context, it should be taken into account a widely accepted notion that the main sources for the scalp-recorded EEG signals derive from the cortex, while the thalamus and the basal ganglia can hardly produce appreciable contribution to the scalp EEG (Nunez, 1995). However, even if a subcortical neural source contributed markedly to scalp-recorded EEG, this deep contribution would be distributed over the source space lying on the cortical surface by the employed model. This phenomenon would result in an increase of the low spatial frequency component in the recorded EEG. If the hypothetical subcortical activation would not be modulated by the performed task, then the computed connectivity patterns will remain unchanged with respect to those not generated by the subcortical sources. This is because the connectivity patterns are statistically compared with respect to the nonsignificant; therefore, given the subcortical activity as not task dependent, its hypothesized contribution will be canceled. Finally, if the subcortical sources contributed effectively to the scalp EEG and were modulated by the performed task, then it would be produced a generalized unspecific increase of correlation between all the ROIs analyzed.

There is a large consensus about the need and usefulness of the multimodal integration of metabolic, neurovascular, and electrophysiological data of neuronal activation also in order to understand their complex interactions in the healthy and diseased brain (see Rossini et al., 2004). The findings reported in the literature (reviewed in Dale and Halgren, 2001) suggest the possibility to improve the spatial details of the estimated neural sources by performing a multimodal integration of EEG or MEG with fMRI. In a recent simulation study, it was found that the use of fMRI priors in the estimation of cortical activity enhances the efficacy of the cortical current density estimation for those ROIs in which fMRI hotspots are located while it does not decrease the cortical current density estimation efficacy for the ROIs with no fMRI hotspots present (Babiloni et al., 2003). In the present study, we have then employed the EEG and fMRI multimodal integration to improve cortical current density estimations in the analyzed ROIs. It is noteworthy that the formulation adopted here to insert the fMRI priors into the estimation of the cortical current density (Eq. (5)) is adequate to support increase as well as decrease of the hemodynamic blood flow underlying the task with respect to the rest period. Indeed, a fMRI prior relative to an increase of the blood flow during the task will cause an increase of the probability for the dipolar source (where the increase is localized) to actively participate to the estimated solution. This is because the cost for its inclusion in the solution decreases, as stated by Eq. (5). The same line of reasoning is applicable for the inclusion of decreased values of fMRI signals with respect to the rest state (negative α_i). In this latter case, the cost for the inclusion of the dipolar source will

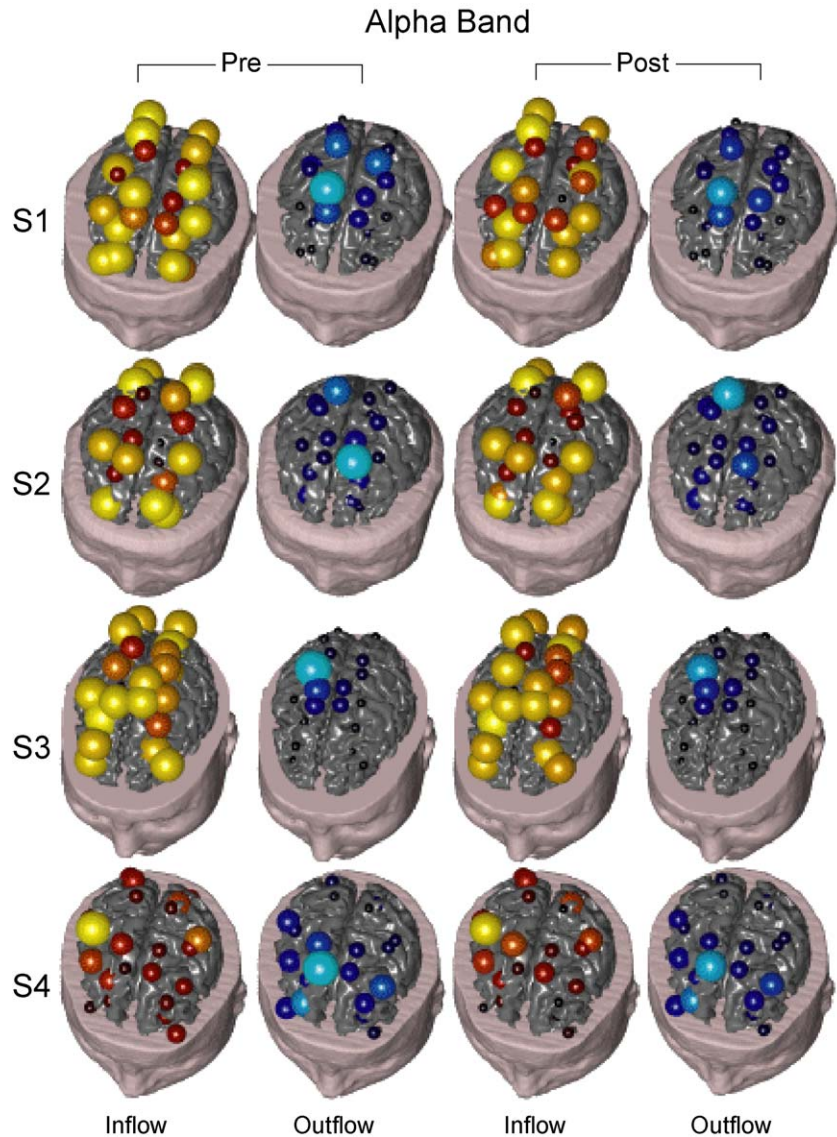


Fig. 6. Figure shows the inflow and outflow patterns obtained for the alpha frequency band from all the ROIs during the PRE and POST periods for all the analyzed subjects. Same conventions of Fig. 2 are applied. Each row is relative to the results obtained in each subject analyzed. The first two columns from left are relative to the PRE time period for the inflow and outflow estimations, while the third and the fourth columns are relative to the POST time period.

increase up to a maximum equal to the inverse of the tuning factor K , and the dipole will not likely be included in the electromagnetic inverse solution estimated by Eq. (3).

Although the locations of neural population generating oscillatory activity have been already estimated with different technologies (Pfurtscheller and Lopes da Silva, 1999; Salmelin et al., 1995; Tesche and Karhu, 2000), the present study addresses the computation of the brain connectivity from the estimated cortical activity. Connectivity measurements among cortical sites have been presented by using MEG recordings (Gross et al., 2001, 2003). The methodology reported in those cases, however, did not allow to immediately recognize the direction of the information flow due to the nondirectional properties of the estimated coherence. In the present study, we have applied a methodology (DTF) already known for the assessment of information flows between scalp electrodes (Kaminski and Blinowska, 1991; Kaminski et al., 2001) to

cortical signals estimated by means of realistic geometry head models and high-resolution EEG recordings.

Additional connectivity estimation techniques are available in neuroscience, besides those discussed above. For instance, the mutual information technique (Inouye et al., 2000) and the cross covariance methodologies (Gevins et al., 1989; Urbano et al., 1998) are able to reveal direct flow of information between one or more scalp electrodes toward another one(s) in the time domain. However, important information in the EEG signals is often coded in the frequency and not in the time domain (reviewed in Pfurtscheller and da Silva, 1999). The DTF is a technique in the frequency domain that has been demonstrated (Kaminski et al., 2001) to rely on the key concept of Granger causality between time series (Granger, 1969): an observed time series $x(n)$ causes another time series $y(n)$ if knowledge of $x(n)$'s past significantly improves prediction of $y(n)$; this relation between time series is not reciprocal, that is, $x(n)$ may cause $y(n)$ without $y(n)$ necessarily causing $x(n)$. This lack of

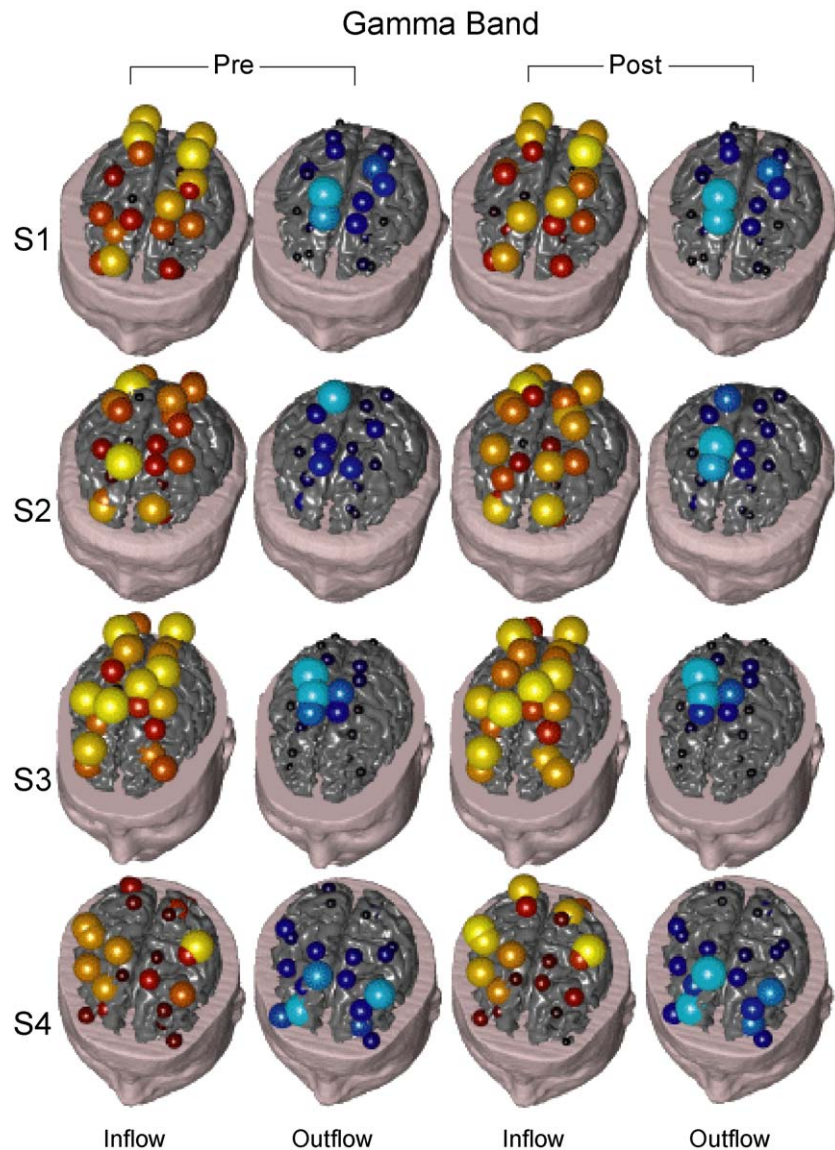


Fig. 7. Inflow and outflow patterns computed for the gamma frequency band. Same conventions as in Fig. 6.

reciprocity permits to evaluate the direction of information flow between structures. With respect to the use of another popular method for the study of cortical connectivity by using hemodynamic measurements, like the Structural Equation Modeling, the DTF does not require the use of a specific cortical connectivity model to be tested. The capability of the DTF methodology to recover connectivity patterns has been already explored in the literature (Kaminski et al., 2001). In addition, a simulation study reported elsewhere has demonstrated as the connectivity estimation performed by DTF is rather robust with respect to systematic variation of signal to noise ratio as well as the length of the recording data (Astolfi et al., 2004). In particular, it has been noted that at least a SNR equals 3 and a LENGTH of the measured cortical data of 45 s are necessary to decrease significantly the errors in the connectivity estimates. Both criteria have been fulfilled by the present EEG recordings.

Our results suggest that the connectivity estimates are quite robust with respect to the optimal choice of the MVAR model order. In fact, Fig. 2 shows that departures from the optimal model order do

not change dramatically the connectivity as well as the outflow pattern of the analyzed data. Substantially, the same information is conveyed by the choice of model order between 5 and 9, although the AIC criterion returned a specifically optimal model order described in Table 1. Moreover, this identity in the connectivity pattern estimated with the different model orders also holds for the other frequency bands examined. The optimal values of the MVAR order range from 6 to 7 in the population analyzed. These values are comparable to the 5 or 6 orders found in EEG models during sleep or isometric muscular contractions (Kaminski et al., 2001; Mima et al., 2001).

It might be argued that the use of constant coefficients for the MVAR model for the connectivity estimates is only justified for the modeling of a stationary process. Here, this issue is addressed by performing the MVAR modeling of the estimated cortical data in two main time segments related to the time period before and after the EMG onset (PRE and POST period). Indeed, it is well known as the cortical information processing substantially differs between movement preparatory phase (PRE period), and the phase when the

somatic feedback from the finger joints is received by the cortex, in the POST period. This difference in the logical information processed by the brain during movement preparation and execution could be reflected by possible variations of the statistical properties of the estimated cortical waveforms. These variations could be viewed as a nonstationarity of the cortical waveforms along the entire time course of the acquired data. We have explicitly tackled this issue by modeling and analyzing separately the data acquired before and after the EMG onset (the PRE and POST time period). We observed minimal changes of the connectivity patterns during the PRE and POST period, as well as a substantial coincidence of the estimated model order was observed for all the subjects in the two time periods, as shown in Table 1.

Application to the real EEG/fMRI data

The described technique has been applied to the ERP data gathered during visually guided finger tapping movements. The main findings obtained with the multimodal integration of ERP and fMRI data are related to the activation of a network involving the right frontoparietal cortical structures. The flow of the connections moves from the parietal and premotor areas toward the right and left prefrontal areas. These results have also been corroborated by the inflow–outflow analysis, indicating how the ROIs located at the parietal (BA 5) and premotor areas (BA 6) could be the source of an activity that spreads and reaches virtually all the other ROIs considered, from the occipital (BA 19) to the prefrontal (BA 9, 46) areas of both hemispheres. No remarkable variations of the inflow–outflow characteristics are noted in both PRE and POST time periods; rather, the same connectivity patterns underlying these two time phases increase or decrease just the strength of the connections.

Beside the highlight on the technology potential, the physiological features of the reported findings are consistent with and further integrate those already known in the literature on finger tapping movements, expressed by both neuroelectric and hemodynamic measurements. In a previous fMRI study, it has been found that the right-sided dorsal premotor cortex was preferentially activated during finger tapping movements together with the bilateral visual cortex, where the visual pacing stimulus was processed (Jäncke et al., 2000). In addition, the same study described a significant activation of the ventral premotor cortex in conjunction with the parietal cortices. These findings yielded to the hypothesis that the bilateral visual activation could trigger the timing of finger movements by transferring the sensory pacing codes via the left and right ‘dorsal’ pathways to the prefrontal cortex, where stimulus response are matched. Of special interest is our observation of the involvement of the occipital area (BA 19) that received information from the ROIs more directly involved in the motor task processing, namely those depicting the premotor and parietal areas. A network including the primary sensorimotor as well as the supplementary motor areas is involved in the execution of visually triggered finger tapping movements, as previously demonstrated by fMRI and PET technologies (Salmelin et al., 1995; Volkman et al., 1996). These latter studies also underlined the role of cerebellum, a role which was not possible to investigate with our noninvasive electrophysiological techniques, due to the large generation of closed potential fields by the cerebellum’s stellate cells that are not detectable by the scalp electrodes. Gerloff et al. (1998) have further underlined the role of the primary sensorimotor and supplementary motor areas in the processing of movement execution based on ERP measurements

from scalp electrodes and the assessment of connectivity with the nondirectional coherence methods.

The connectivity patterns of the premotor and prefrontal ROIs reported here are in agreement with earlier electromagnetic findings, suggesting that the dorsolateral and the ventral premotor cortices are the specific candidate for movement execution guided by sensory information as opposed to movements carried out with no sensory control (Classen et al., 1998; Rothwell et al., 1991; Sekihara and Scholz, 1996). Finally, the present activity noted in the parietal area (BA 5) could reflect the role that such area has in the somatosensory-motor integration for motor actions. Indeed, it has been hypothesized that such area could be regarded as a higher-order somatosensory zone devoted to the analysis of proprioceptive information from joints for the appropriate motor control (Rizzolatti et al., 1998).

In conclusion, we have presented here an integrated approach to estimate brain cortical connectivity information by using non-invasive methodologies involving the multimodal integration of electrophysiological and hemodynamic measurements. These methodologies enable us to detect the level of statistical significance of the estimated cortical activations in the selected ROIs and to follow the time-varying pattern of connectivity eventually developing during simple motor tasks in humans. This body of methodologies can be suitable for the analysis of simple as well as complex movements or cognitive tasks in humans.

Acknowledgments

This work was partially supported by grant NSF BES-0218736 and by a grant from the IRIB Program.

References

- Abt, K., 1983. Significance testing of many variables. *Problems and solutions. Neuropsychobiology* 9 (1), 47–51.
- Astolfi, L., Babiloni, F., Babiloni, C., Carducci, F., Cincotti, F., Basilisco, A., Rossini, P.M., Salinari, S., Ding, L., Ni, Y., He, B., 2004. Assessing time-varying cortical connectivity by high resolution EEG and directed transfer function: simulations and application to finger tapping data. 26th IEEE-EMBS International Conference, San Francisco, pp. 1–4 (September).
- Babiloni, F., Babiloni, C., Carducci, F., Fattorini, L., Anello, C., Onorati, P., Urbano, A., 1997. High resolution EEG: a new model-dependent spatial deblurring method using a realistically shaped MR-constructed subject’s head model. *Electroencephalogr. Clin. Neurophysiol.* 102 (2), 69–80.
- Babiloni, F., Babiloni, C., Locche, L., Cincotti, F., Rossini, P.M., Carducci, F., 2000. High-resolution electroencephalogram: source estimates of Laplacian-transformed somatosensory-evoked potentials using a realistic subject head model constructed from magnetic resonance images. *Med. Biol. Eng. Comput.* 38 (5), 512–519.
- Babiloni, F., Babiloni, C., Carducci, F., Romani, G.L., Rossini, P.M., Angelone, L.M., Cincotti, F., 2003. Multimodal integration of high-resolution EEG and functional magnetic resonance imaging data: a simulation study. *NeuroImage* 19 (1), 1–15.
- Brovelli, P., Battaglini, J., Naranjo, R., 2002. Medium-range oscillatory network and the 20-hz sensorimotor induced potential. *NeuroImage* 16 (1), 130–141.
- Buchel, C., Friston, K.J., 1997. Modulation of connectivity in visual pathways by attention: cortical interactions evaluated with structural equation modelling and fMRI. *Cereb. Cortex* 7 (8), 768–778.
- Classen, J., Gerloff, C., Honda, M., Hallett, M., 1998. Integrative visuomotor

- behavior is associated with interregionally coherent oscillations in the human brain. *J. Neurophysiol.* 3, 1567–1573.
- Dale, A.M., Sereno, M., 1993. Improved localization of cortical activity by combining EEG and MEG with MRI cortical surface reconstruction: a linear approach. *J. Cogn. Neurosci.* 5, 162–176.
- Dale, A.M., Halgren, E., 2001. Spatiotemporal mapping of brain activity by integration of multiple imaging modalities. *Curr. Opin. Neurobiol.* 11 (2), 202–208.
- Dale, A., Liu, A., Fischl, B., Buckner, R., Belliveau, J.W., Lewine, J., Halgren, E., 2000. Dynamic statistical parametric mapping: combining fMRI and MEG for high-resolution imaging of cortical activity. *Neuron.* 26, 55–67.
- David, O., Cosmelli, D., Friston, K.J., 2004. Evaluation of different measures of functional connectivity using a neural mass model. *NeuroImage* 21, 659–673.
- Gerloff, Richard, C.J., Hadley, J., Schulman, A. E., Honda, M., Hallett, M., 1998. Functional coupling and regional activation of human cortical motor areas during simple, internally paced and externally paced finger movements. *Brain* 121, 1513–1531.
- Gevens, A., 1989. Dynamic functional topography of cognitive task. *Brain Topogr.* 2, 37–56.
- Gevens, A.S., Cuttillo, B.A., Bressler, S.L., Morgan, N.H., White, R.M., Illes, J., Greer, D.S., 1989. Event-related covariances during a bimanual visuomotor task II. Preparation and feedback. *Electroencephalogr. Clin. Neurophysiol.* 74, 147–160.
- Gevens, A., Brickett, P., Reutter, B., Desmond, J., 1991. Seeing through the skull: advanced EEGs use MRIs to accurately measure cortical activity from the scalp. *Brain Topogr.* 4, 125–131.
- Gevens, A., Le, J., Leong, H., McEvoy, L.K., Smith, M.E., 1999. Deblurring. *J. Clin. Neurophysiol.* 16 (3), 204–213.
- Granger, C.W.J., 1969. Investigating causal relations by econometric models and cross-spectral methods. *Econometrica* 37, 424–428.
- Grave de Peralta Menendez, R., Gonzalez Andino, S.L., 1999. Distributed source models: standard solutions and new developments. In: Uhl, C. (Ed.), *Analysis of Neurophysiological Brain Functioning*. Springer, pp. 176–201.
- Grinvald, A., Lieke, E., Frostig, R.D., Gilbert, C.D., Wiesel, T.N., 1986. Functional architecture of cortex revealed by optical imaging of intrinsic signals. *Nature* 324 (6095), 361–364.
- Gross, Kujala, J., Hämäläinen, M., Timmermann, L., Schnitzler, A., Salmelin, R., 2001. Dynamic imaging of coherent sources: studying neural interactions in the human brain. *Proc. Natl. Acad. Sci. U. S. A.* 98 (2), 694–699.
- Gross, J., Timmermann, L., Kujala, J., Salmelin, R., Schnitzler, A., 2003. Properties of MEG tomographic maps obtained with spatial filtering. *NeuroImage* 19 (4), 1329–1336.
- Hämäläinen, M., Ilmoniemi, R., 1984. *Interpreting Measured Magnetic Field of the Brain: Estimates of the Current Distributions*. Technical Report TTK-F-A559, Helsinki University of Technology.
- Hansen, P.C., 1992a. Analysis of discrete ill-posed problems by means of the L-curve. *SIAM Rev.* 34, 561–580.
- Hansen, P.C., 1992b. Numerical tools for the analysis and solution of Fredholm integral equations of the first kind. *Inverse Probl.* 8, 849–872.
- He, B., Lian, J., 2002. Spatio-temporal functional neuroimaging of brain electric activity. *Crit. Rev. Biomed. Eng.* 30, 283–306.
- He, B., Zhang, Z., Lian, J., Sasaki, H., Wu, S., Towle, V.L., 2002. Boundary element method based cortical potential imaging of somatosensory evoked potentials using subjects' magnetic resonance images. *NeuroImage* 16, 564–576.
- Horwitz, B., 2003. The elusive concept of brain connectivity. *NeuroImage* 19, 466–470.
- Inouye, T., Iyama, A., Shinosaki, K., Toi, S., Matsumoto, Y., 1995. Inter-site EEG relationships before widespread epileptiform discharges. *Int. J. Neurosci.* 82, 143–153.
- Jäncke, R., Loose, K., Luta, K., Specht, N., Shah, J., 2000. Cortical activations during paced finger-tapping applying visual and auditory pacing stimuli. *Cogn. Brain Res.* 10 (1–2), 51–66.
- Kaminski, Blinowska, K.J., 1991. A new method of the description of the information flow in the brain structures. *Biol. Cybern.* 65, 203–210.
- Kaminski, M., Ding, M., Truccolo, W.A., Bressler, S., 2001. Evaluating causal relations in neural systems: granger causality, directed transfer function and statistical assessment of significance. *Biol. Cybern.* 85, 145–157.
- Lee, L., Harrison, L.M., Mechelli, A., 2003. The functional brain connectivity workshop: report and commentary. *NeuroImage* 19, 457–465.
- Liu, A.K., 2000. *Spatiotemporal Brain Imaging*, PhD dissertation. Massachusetts Institute of Technology, Cambridge, MA.
- Liu, A.K., Belliveau, J.W., Dale, A.M., 1998. Spatiotemporal imaging of human brain activity using functional MRI constrained magnetoencephalography data: Monte Carlo simulations. *Proc. Natl. Acad. Sci.* 95 (15), 8945–8950.
- Logothetis, N.K., Pauls, J., Augath, M., Trinath, T., Oeltermann, A., 2001. Neurophysiological investigation of the basis of the fMRI signal. *Nature* 412 (6843), 150–157.
- Magistretti, P.J., Pellerin, L., Rothman, D.L., Shulman, R.G., 1999. Energy on demand. *Science* 283 (5401), 496–497.
- McIntosh, A.R., Gonzalez-Lima, F., 1994. Structural equation modelling and its application to network analysis in functional brain imaging. *Brain Mapp.* 2, 2–22.
- Mima, T., Matsuoka, T., Hallett, M., 2001. Information flow from the sensorimotor cortex to muscle in humans. *Clin. Neurophysiol.* 112 (1), 122–126.
- Moretti, D.V., Babiloni, F., Carducci, F., Cincotti, F., Remondini, E., Rossini, P.M., Salinari, S., Babiloni, C., 2003. Computerized processing of EEG-EOG-EMG artifacts for multi-centric studies in EEG oscillations and event-related potentials. *Int. J. Psychophysiol.* 47 (3), 199–216.
- Nunez, P., 1981. *Electric Fields of the Brain*. Oxford Univ. Press, New York.
- Nunez, P.L., 1995. *Neocortical Dynamics and Human EEG Rhythms*. Oxford Univ. Press, New York.
- Pascual-Marqui, R.D., 1995. Reply to comments by Hamalainen, Ilmoniemi and Nunez. *Skrandies, W. ISBET NewsL.*, vol. 6., pp. 16–28. December.
- Pfurtscheller, G., Lopes da Silva, F.H., 1999. Event-related EEG/MEG synchronization and desynchronization: basic principles. *Clin. Neurophysiol.* 110 (11), 1842–1857.
- Puce, A., Allison, T., Spencer, S.S., Spencer, D.D., McCarthy, G., 1997. Comparison of cortical activation evoked by faces measured by intracranial field potentials and functional MRI: two case studies. *Hum. Brain Mapp.* 5 (4), 298–305.
- Rizzolatti, G., Luppino, G., Matelli, M., 1998. The organization of the cortical motor system: new concepts. *Electroencephalogr. Clin. Neurophysiol.* 106, 283–296.
- Rossini, P.M., Altamura, C., Feretti, A., Vernieri, F., Zappasodi, F., Caulo, M., Pizzella, V., Del Gratta, C., Romani, G.-L., Tecchio, F., 2004. Does cerebrovascular disease affect the coupling between neuronal activity and local haemodynamics? *Brain* 127, 99–110 (Jan).
- Rothwell, J., Thompson, P., Day, B., Boyd, S., Marsden, C., 1991. Stimulation of the human motor cortex through the scalp. *Exp. Physiol.* 76, 159–200.
- Salmelin, R., Hämäläinen, M., Kajola, M., Hari, R., 1995. Functional segregation of movement-related rhythmic activity in the human brain. *NeuroImage* 2, 237–243.
- Schlosser, R., Gesierich, T., Kaufmann, B., Vucurevic, G., Hunsche, S., Gawehn, J., Stoeter, P., 2003. Altered effective connectivity during working memory performance in schizophrenia: a study with fMRI and structural equation modeling. *NeuroImage* 19 (3), 751–763.
- Sekihara, K., Scholz, B., 1996. Generalized Wiener estimation of three-dimensional current distribution from biomagnetic measurements. *IEEE Trans. Biomed. Eng.* 43 (3), 281–291.
- Taniguchi, M., Kato, A., Fujita, N., Hirata, M., Tanaka, H., Kihara, T., Ninomiya, H., Hirabuki, N., Nakamura, H., Robinson, S.E., Cheyne,

- D., Yoshimine, T., 2000. Movement-related desynchronization of the cerebral cortex studied with spatially filtered magnetoencephalography. *NeuroImage* 12 (3), 298–306.
- Tesche, C., Karhu, J., 2000. Theta oscillations index human hippocampal activation during a working memory task. *Proc. Natl. Acad. Sci. U. S. A.* 97, 919–924.
- Theiler, J., Eubank, S., Longtin, A., Galdrikian, B., Farmer, J.D., 1992. Testing for nonlinearity in time series: the method of surrogate data. *Physica D* 58, 77–94.
- Urbano, A., Babiloni, C., Onorati, P., Babiloni, F., 1998. Dynamic functional coupling of high resolution EEG potentials related to unilateral internally triggered one-digit movements. *Electroencephalogr. Clin. Neurophysiol.* 106 (6), 477–487.
- Volkman, J., Joliot, M., Mogilner, A., Ioannides, A., Lado, F., Fazzini, E., Ribary, U., Llinas, R., 1996. Central motor loop oscillations in parkinsonian resting tremor revealed by magnetoencephalography. *Neurology* 46, 1359–1370.
- Zar, J., 1984. *Biostatistical Analysis*. Prentice-Hall.